Received: 9 September 2022 | Revised: 26 August 2023 | Accepted: 12 September 2023

DOI: 10.1111/geb.13765

Global Ecology and Biogeography | A Journal of Macroecology

WILEY

RESEARCH ARTICLE

The biogeography of embolism resistance across resource gradients in the Amazon

Maquelle N. Garcia[1] | Tomas F. Domingues[2] | Rafael S. Oliveira[3] | Flávia R. C. Costa[4]

[1]Programa de pós graduação em Ciências de Florestas Tropicais, Instituto Nacional de Pesquisas da Amazônia, Manaus, Brazil

[2]Departamento de biologia, Faculdade de Filosofia, Ciências e Letras de Ribeirão Preto, Universidade de São Paulo, Ribeirão Preto, Brazil

[3]Departamento de Biologia Vegetal, Instituto de Biologia, Universidade Estadual de Campinas, Campinas, Brazil

[4]Coordenação de Pesquisas em Biodiversidade, Instituto Nacional de Pesquisas da Amazônia, Manaus, Brazil

Correspondence
Maquelle N. Garcia, Programa de pós graduação em Ciências de Florestas Tropicais, Instituto Nacional de Pesquisas da Amazônia, CEP 69008-971, Manaus, AM, Brazil.
Email: maquelleneves@gmail.com

Funding information
Conselho Nacional de Desenvolvimento Científico e Tecnológico, Grant/Award Number: 441282/2016-4 and 403764/2012-2; PEER Program, Grant/Award Number: AID-OAA-A-11-00012; PELD, Grant/Award Number: 558244/2009-2; FAPEAM PROFIX-RH, Grant/Award Number: 01.02.016301.00411/2022-52

Handling Editor: Naia Morueta-Holme

Abstract

Aim: Understanding tree mortality under climate change-induced droughts requires knowledge of hydraulic trait distribution across environmental gradients. The spatial distribution of embolism resistance (i.e., P50), a key trait linked to hydraulic failure, is currently unknown across the Amazon. Here, we tested how precipitation, water table depth (WTD) and soil fertility interact as filters modulating the geographic hydraulic trait distribution.

Location: Four sites in three key regions across the Amazon basin: Central, Western peripheral area and Brazilian Shield.

Time Period: Present.

Major Taxa Studied: Tree species.

Method: We measured hydraulic vulnerability curves of 64 tree species (165 individuals) using an orthogonal design contrasting seasonal precipitation gradients, soil fertility and WTD. To estimate the geographical distribution of hydraulic traits for the basin scale, we use the coefficients of the best generalized linear model, projected on a 1 km grid in each environmental layer.

Results: We show that WTD and soil fertility are the main drivers of embolism resistance, while precipitation has a secondary effect. Trees in shallow WTD and fertile soils had riskier hydraulic strategies. Our spatial projection identified the Amazonian southern band and valleys across the basin as the most vulnerable areas. High soil fertility in these regions increases the variability of hydraulic traits and thus uncertainty in predictions of drought responses.

Main Conclusion: At the scale of the Amazon basin, we show that dominant tree species traits converge toward hydraulic resistance when resource (water and nutrients) levels are low and towards hydraulic vulnerability (but with higher trait variability) when resources increase. These results highlight the importance of WTD and soil fertility in structuring hydraulic traits and their effects on tree mortality under climate change-induced droughts. Further empirical tests covering a wider spatial range and more tree species will help validate our biogeographical distribution model.

KEYWORDS
economic traits, functional traits, hydraulic failure, tree mortality, tropical trees

1 | INTRODUCTION

Recent studies have documented increased drought-driven tree mortality in the Amazon (McDowell et al., 2018; Phillips et al., 2009). However, the probability of death is highly variable across forest environments and species (Esquivel-Muelbert et al., 2020). Thus, predicting the likelihood of tree mortality remains a complex challenge (Brodribb et al., 2020; McDowell, 2011; McDowell et al., 2008; Trugman et al., 2021). Under extreme water deficits, the increase in xylem embolism can lead to hydraulic failure and, eventually, tree death. The dominant plant hydraulic traits and strategies and their variations are selected according to the long-term environment to which trees are exposed (Grime, 1977). Hydraulic traits provide the substrate for tree responses to climate change and thus may determine the future of forests; however, their distribution and drivers across Amazonia are only recently starting to unfold (Tavares et al., 2023). Despite recent progress, critical factors known to affect those traits at local scale, such as groundwater and the interaction of resources—water and nutrients, have not yet been examined at the basin scale. In this study, we seek to narrow this gap by understanding the drivers of plant hydraulics at the scale of the Amazon basin and proposing a map of their distribution.

The physiological mechanism behind hydraulic failure involves water movement in plants. The regulation of stomatal conductance controls leaf CO_2 uptake and water loss by transpiration (Sperry, 2000). As transpiration and tension in the water column increase, the risk of cavitation and embolism formation (filling of the vessel elements with air) also increases, compromising the xylem vessel functionality (Zwieniecki & Secchi, 2015). Evergreen trees usually exhibit three main strategies to maintain functionality during drought: (1) closure of stomata as soil water potentials start decreasing, to prevent wilting and increased xylem embolism (Garcia, Ferreira, et al., 2021); (2) investing in higher embolism resistance (Anderegg et al., 2016; Powers et al., 2020); and (3) accessing water in the soil through deep rooting (Brum et al., 2019; Rutuja et al., 2021). Alternatively, species lacking any strategy to cope with drought may be restricted to growing in places where soil water availability is high (Oliveira et al., 2019; Silvertown et al., 2015). Ecophysiological studies should consider integrating these three strategies to provide a more comprehensive understanding of tree drought response. However, combining measurements of stomatal control, hydraulics and rooting depth during droughts is expensive, and this information is still lacking for Amazonian forests. Thus, broadening our understanding of tree drought-tolerance strategies, such as variation in embolism resistance and hydrological environments, can be a first step to honing our predictions of Amazon forest response to climate change (Powers et al., 2020; Rowland et al., 2015). Vulnerability to embolism can be experimentally assessed from the relationships between leaf water potential and the xylem percent loss of conductivity, P12, P50 and P88. The initial onset of cavitation (P12) is the tension of the xylem water column (water potential) at which pit membranes within the conducting xylem are overcome with air (Sparks & Black, 1999). P12 corresponds to the period during which plants actively regulate leaf stomata to reduce water loss and prevent the propagation of cavitation (Garcia, Ferreira, et al., 2021; Sorek et al., 2021). P50 is the water potential at which 50% of water conductivity is lost and represents incipient damage to plant functionality (Skelton et al., 2018). P88 is the water potential associated with canopy dieback in angiosperms (Urli et al., 2013).

Recently, Oliveira et al. (2021) proposed an axis of trait covariation involving carbon acquisition and water loss, according to resource gradients (precipitation and soil fertility). On large—global to regional—scales, low precipitation has been shown to select high embolism resistance (Choat et al., 2012). Tavares et al. (2023) show that forests with fast-growing species take greater hydraulic risks and face greater mortality risk. Additionally, fast-growing plants on nutrient-rich soils are expected to have lower hydraulic safety margins than slow-growing plants on nutrient-poor soils, in accordance with the fast–slow plant economic spectrum that integrates across leaves, stems and roots to explain species' ecological strategies (Reich, 2014). The extremes of the continuous variation along this integrated precipitation and soil fertility resource axis are proposed to be the fast-growth-risky hydraulics and slow-growth-secure hydraulic strategies (Guillemot et al., 2022; Oliveira et al., 2021). However, there is also evidence showing that the coordination of traits related to hydraulics, light and nutrient acquisition can be weak or decoupled (Baraloto et al., 2010; Gleason et al., 2016; Liu et al., 2021; Maréchaux et al., 2015). It can be argued that this lack or weak coordination may be a symptom of the lack of coverage of large enough resource gradients to disclose the patterns since even the economic spectrum itself is clear at large scales but noisy at small ones (Wright et al., 2007). This is an important topic we directly investigate here since the existence of greater coordination would simplify modelling efforts.

Besides precipitation and soil fertility, root access to deep soil water can also affect hydraulic systems locally. The water availability to plants depends on the combination of precipitation and access to deep sources such as the water table, and this combination may produce a steady water supply even under the dry season (the extreme example being oases). Thus, any simple description of water supply based only on precipitation, or indices derived from that, will not capture its fine-grained structure affecting plant traits. At the local scale, it has been shown that trees growing in areas with shallow water tables have low embolism resistance, and conversely, those on deep water tables have high embolism resistance (Garcia, Hu, et al., 2021; Oliveira et al., 2019). About 50% of the Amazon forests occur in shallow water table depth (<5 m) (Costa et al., 2023). For these reasons, a realistic projection of the abundance of fast-growth-risky and slow-growth-secure hydraulic strategies must consider the integrated roles of precipitation, soil fertility and water table depth. During normal seasonal conditions in the Amazon, trees growing in deep water table areas have lower mortality and higher productivity than those in shallow water table areas (Sousa et al., 2022). On the other hand, during moderate droughts, mortality can be buffered, and productivity increases in shallow water tables (Costa et al., 2023). However, how these relationships co-vary/

interact with soil fertility is currently unknown. Comprehending this co-variation will help understanding if the same growth strategies select hydraulic traits.

This study integrates these three factors (soil fertility, precipitation and water table depth) in a fully nested design to advance knowledge of the drivers and distribution of hydraulic tree strategies across environmental gradients. These results are then used to map the distribution of tree hydraulics strategies and predict the Amazon Forest response to drought. We pose three questions: (1) How do climatic water deficit, soil fertility and water table depth affect P12, P50 and P88 across the Amazon? We hypothesize that precipitation deficit will be the primary driver of plant hydraulic resistance, as shown in large-scale studies, while fertility and water table depth will have secondary effects. Specifically, lower precipitation will be associated with plants with higher P12, P50 and P88, irrespective of soil fertility. In contrast, plants growing in wet climates with high fertility will exhibit low embolism resistance, and those growing in moist sites with low fertility will show intermediate embolism resistance. (2) Is there a difference in the predictive power of each environmental factor among different hydraulic resistance metrics, which could indicate differences in hydraulic strategies during a drought? We hypothesize that the initial phase of the cavitation process (P12), which may be associated with stomatal control, will be more closely related to soil fertility and precipitation water deficit. Meanwhile, P50 and P88 are expected to be more significantly influenced by variables linked to soil water availability and climatic water deficit, as shown by other studies we discussed above. Finally, we ask whether statistical models of hydraulic trait dependence on water and nutrients can be combined with gridded and remote sensing observations to generate meaningful basin-wide maps of embolism resistance. We test the plausibility of such maps by comparing them to existing spatially distributed data on tree mortality to determine whether such mapping can increase our understanding of patterns of forest vulnerability to climate change.

2 | RESULTS

We tested models predicting hydraulic traits' responses from patterns of key biogeochemical gradients across the basin, including soil fertility (Phosphorus [P] and exchangeable base cations), water table depth (WTD) and climatic water deficit (maximum cumulative water deficit, MCWD). We also tested the inclusion of species and sites as random factors, with no noticeable improvement over simpler models (Tables S3 and S4). The inclusion of species as a random factor improved the fit of the best models for P12, P50 and P88. However, the inclusion of sites did not improve the fit of most models, especially those using phosphorus as the fertility variable (Tables S5 and S6). We detected that soil fertility considering P and water table depth had, on average, stronger effects on hydraulic resistance metrics than the climatic water deficit (Table 1). The soil fertility effect is stronger on P12 and P50 in interaction with MCWD, while P88 is driven only by water table depth and soil fertility (Figure 1).

TABLE 1 Results of the GLM models (ΔAIC < 2) considering water table depth (WTD); maximum climatological water deficit (MCWD); and soil fertility represented by phosphorus (P) as predictors of the water potential point indicating the start of cavitation (P12), the water potential at which 50% of conductivity is lost (P50) and the water potential point associated with dieback (P88).

Independent var	Dependent var	Intercept	WTD	P	MCWD	MCWD:P	WTD:P	WTD:MCWD	R^2	AICc	ΔAICc
WTD, MCWD, P	P12	+0.91***	+0.17*	−0.09 ns	−0.23*	−0.63**	-	-	0.18	244.4	0
WTD, MCWD, P	P50	+0.73***	+0.23***	−0.21**	−0.14 ns	−0.43*	-	-	0.27	308.4	0
WTD, MCWD, P	P50	+0.73***	+0.23***	−0.19*	−0.14 ns	−0.40*	−0.05 ns	-	0.27	310	1.6
WTD, MCWD, P	P50	+0.61***	+0.25***	−0.30***	-	-	-	-	0.22	310.4	1.97
WTD, MCWD, P	P50	+0.74***	+0.25**	−0.22**	−0.13 ns	−0.45**	-	+0.05 ns	0.27	310.4	1.99
WTD, MCWD, P	P88	+1.5***	+0.23***	−0.15**	-	-	-	-	0.13	513.8	0
WTD, MCWD, P	P88	+1.5***	+0.23***	−0.17**	-	-	+0.03 ns	-	0.13	515.8	1.96

Note: The numbers associated with each variable represent their standardized regression coefficients. Codes: '***' 0.001; '**' 0.01; '*' 0.05; 'ns' not significant; '+' positive effect; '−' negative effect; '-' variable not included in the model.

Abbreviations: AIC, Akaike's information criterion; R^2, likelihood ratio based.

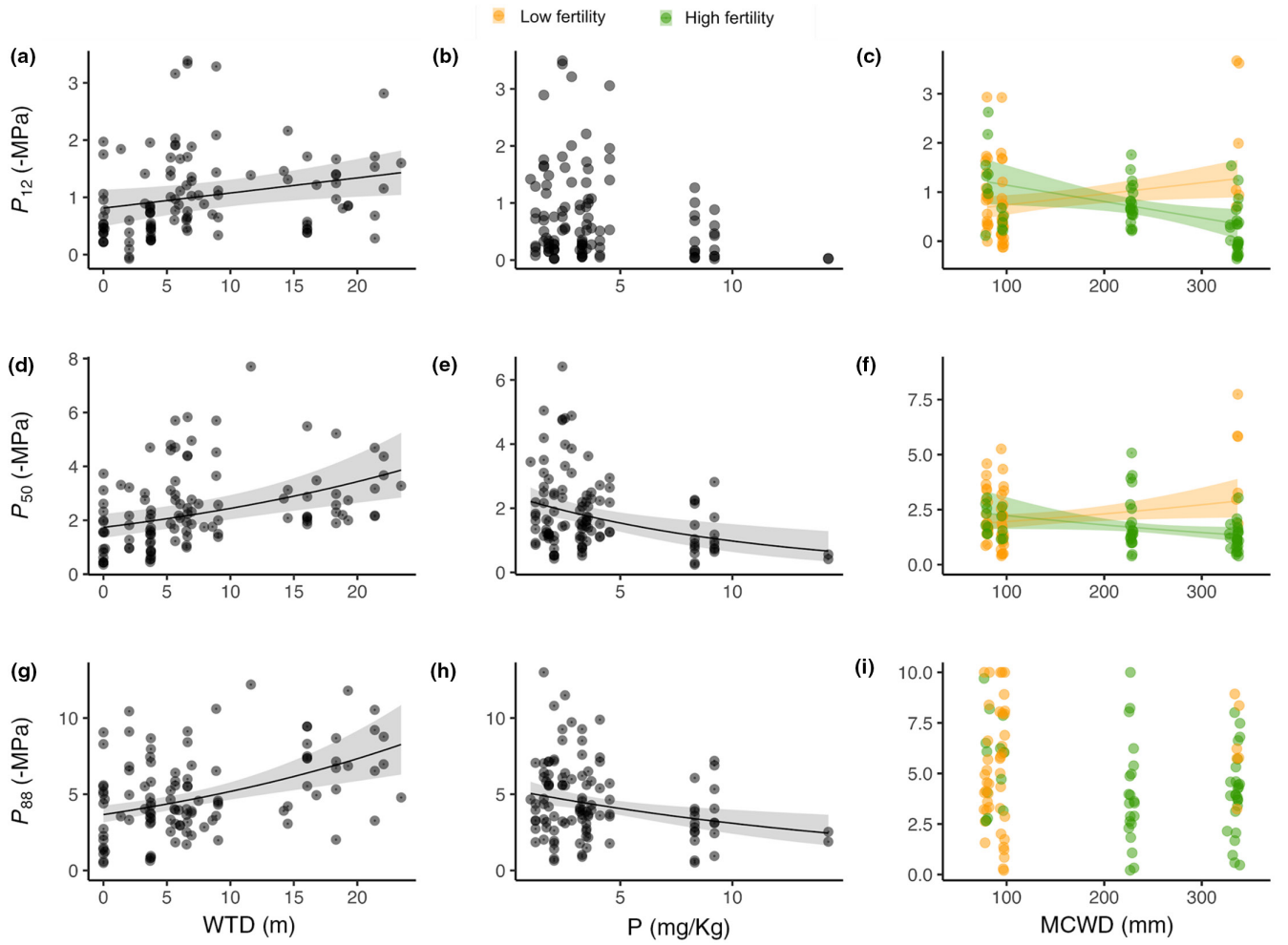

FIGURE 1 Partial effects of predictors on individual tree hydraulic traits in the best statistical models (ΔAICc = 0; Table 1) for (a–c) water potential point indicating the start of cavitation (P12); (d–f) water potential at which 50% loss of conductivity is lost (P50); and (g–i) water potential point associated with dieback (P88). The predictor variables are water table depth (WTD, left column), phosphorus (P, middle column) and maximum cumulative water deficit (MCWD, right column), where greater deficits indicate drier conditions. The colours represent soil fertility as phosphorus concentration, with low <4.53 < high (mg/kg). The fitted lines with shaded uncertainty bands represent statistically significant partial effects from the best models, and the absence of a line indicates lack of statistical significance with respect to the independent variable. Interaction effects are indicated by coloured lines with coloured shades.

A deep-water table positively affects P12, and as such, selects for a safer hydraulic system (Figure 1a). In contrast, we observed that MCWD not only has a negative average effect on P12 (Table 1), but also interacts with phosphorus, meaning that the precipitation effect is largely mediated by the phosphorus concentration. Phosphorus did not have an average effect on P12 apart from the interaction (Figure 1b). Surprisingly, this interaction indicates that plants have low embolism resistance in dry areas when combined with high phosphorus. We observed the opposite response in dry conditions and low phosphorus fertility areas, where plants exhibited high embolism resistance (Figure 1c). The responses are similar for P50, with hydraulic resistance increasing with WTD (Figure 1d); however, the effect of WTD is more robust than for P12. The average effect of phosphorus concentration on P50 is negative (Figure 1e), meaning that hydraulic resistance decreases with higher fertility. The interaction of MCWD and phosphorus is also present in the best model for P50, with the same trends described for P12 (Figure 1f). P88 increases with WTD (Figure 1g) and decreases with phosphorus (Table 1, Figure 1h), but there is no direct effect of MCWD or interaction between MCWD and phosphorus (Figure 1i). MCWD contributes a high relative weight to the prediction of P12 across the set of all models (0.94), but this reduces to (0.81) in the prediction of P50 and is even lower (0.47) for P88. The water table depth has a relatively constant and high weight as a predictor of P12 (0.91), P50 (0.99) and P88 (0.99). Fertility also has similarly high relative weight as a predictor of P12 (0.99), P50 (0.99) and P88 (0.90).

Models representing soil fertility through exchangeable cations (rather than phosphorus) provided similar results as those presented above. In this case, however, soil fertility interacted with either WTD or MCWD in its effects on P12 and P50, respectively (Table S2).

The phylogenetic signal tested by Blomberg's *K* returned values below <1, suggesting that phylogenetically closer species have less similar traits than expected by the Brownian model of trait evolution, as seen in the mapping of traits along the phylogeny (Figure S7).

However, none of the *K* values was significant (P50 $K=0.17$, $p=0.37$; P12 $K=0.25$, $p=0.17$; P88 $K=0.20$, $p=0.22$. $K<1$ and $p>0.001$), indicating that those traits were neither phylogenetically conserved nor dispersed at the scale of this study. This supports our model's findings of environmental selection of trait values.

The spatial patterns of hydraulic vulnerability projected from our models (Figure 2) strongly reflect the macroscale spatial patterns of soil fertility. Areas with the highest vulnerability to embolism are associated with more fertile regions, mostly in the southern band of the Amazon basin and crossing medium WTD and high MCWD conditions to deep WTD and high MCWD in the south-east. The areas with the highest hydraulic resistance are associated with deep water tables and infertile soils in the Guiana and Brazilian shields. The combined effect of the shallow water table and low fertility resulted in intermediate resistance to embolism from the central to the south-western portions of the basin. The patterns of low-to-medium hydraulic resistance linked to shallow WTD show up along major river channels, but mainly over the macroscale pattern set by soil fertility. Small valleys also follow this same pattern, but we cannot differentiate the detailed patterns associated with WTD at the scale of this map.

We found a significant relationship between the mortality rates from Esquivel-Muelbert et al. (2020) with P88 ($p=0.007$; Figure 2a, insertion), P50 ($p<0.001$; Figure 2b, insertion) and P12 ($p<0.001$; Figure 2c, insertion). This result brings evidence that our modelled embolism resistance correlates well with the observed average mortality rates in the Amazon.

Given that hydraulic resistance is mainly affected by a combination of WTD and soil fertility, we used these factors in combination to examine the variation in hydraulic resistance distributions (Figure 3). The frequency distributions of P12, P50 and P88, according to the

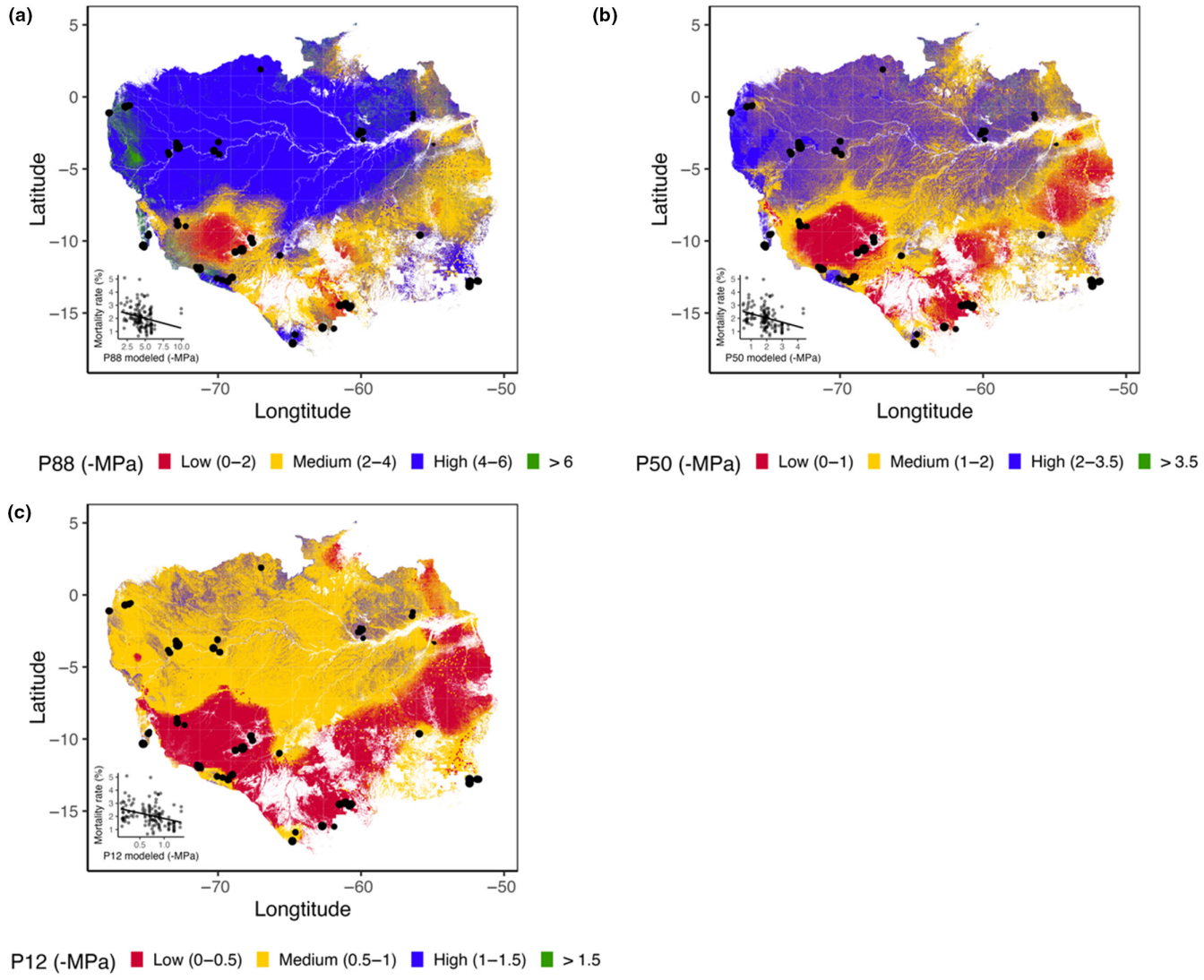

FIGURE 2 Embolism resistance modelled along the basin. (a) P12, (b) P50 and (c) P88. Black circles are indicating sites with annual mortality rate data (*source*: Esquivel-Muelbert et al., 2020). The circle size is proportional to the mortality rate. The graphs inserted in a–c represent the relationship between mortality and P12, P50 and P88, respectively, shown as black circles. Regression lines in black represent the relationship between mortality rates from Esquivel-Muelbert et al. (2020) and P88 ($p=0.007$); P50 ($p<0.001$); and P12 ($p<0.001$). The maps were generated using the coefficients from the models shown in Table S2; in the basin-scale section (bottom).

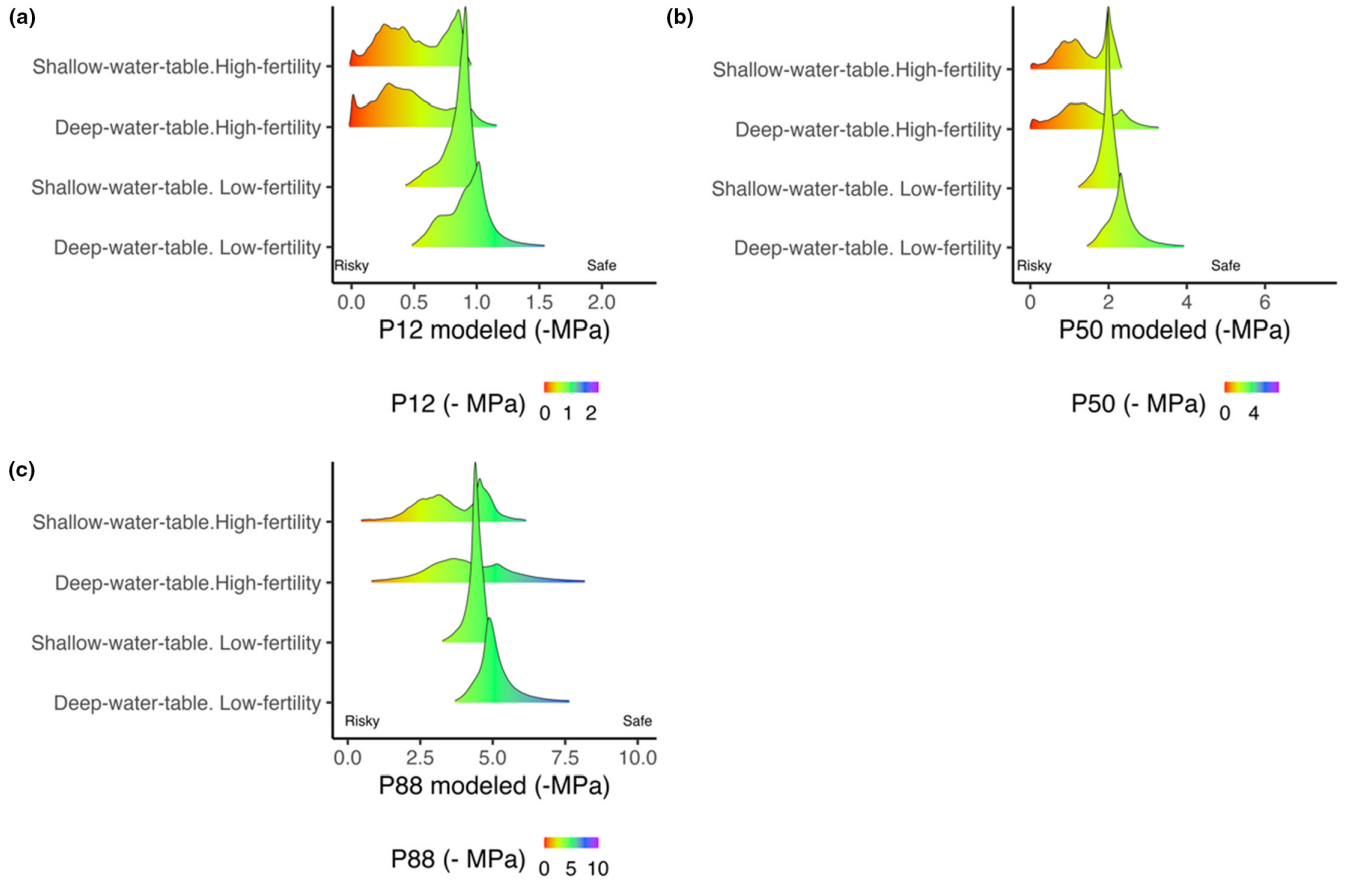

FIGURE 3 Distribution of modelled embolism resistance values for (a) P12; (b) P50; and (c) P88 across the Amazon, grouped by soil fertility and water table depth. Soil fertility is categorized as exchangeable cations concentration >1.21 cmol/kg, and water table depth as deep >5 m.

combinations of soil fertility and water table depth, show that high fertility, irrespective of WTD selects a high diversity of hydraulic resistance values (vulnerable-to-moderately safe trees). High fertility combined with shallow water table depth increases the frequency of riskier hydraulic systems. In contrast, nutrient-poor soils with deeper water tables generate safer hydraulic systems with an even less diverse hydraulic distribution.

3 | DISCUSSION

The Amazon has vast environmental heterogeneity, which is expected to generate diverse and complex tree responses to the increasingly common climate change-driven droughts. Separate pieces of evidence indicate that variations in precipitation, hydrology and soil fertility can affect plant hydraulic resistance and thus affect their responses to drought. For the first time, we tested how these factors interact as filters in this study, modulating the hydraulic traits distribution of Amazonian Forest trees. The four main findings that emerged from our research were as follows: (1) shallow water table depth and high soil fertility are the main drivers of vulnerable hydraulic systems across the Amazon, while the precipitation effects depend on interactions with soil fertility (Figure 1). (2) The effects of environmental drivers differ along the embolism resistance trees, and soil fertility drives P12 and P50 to diverge between places within the same climate water deficit, while P88, by contrast, is determined exclusively by WTD and fertility. (3) The spatial projection of hydraulic traits over the Amazon basin indicates a large southern band as the most hydraulically vulnerable region, primarily due to fertile soils, and shallow water tables create fine-scale variation in vulnerability across the other regions (Figure 2). (4) There is a large diversity of hydraulic traits, especially within high-fertility soils (Figure 3).

Water table depth and fertility were better predictors of embolism resistance than average climatic water deficit, even when MCWD was controlled in multiple regression models. A previous study comparing 11 Amazonian sites found that central Amazon species are resistant while western Amazon species show markedly lower hydraulic resistance, and the most vulnerable region is southern (Tavares et al., 2023). However, that study did not simultaneously control soil fertility, which might affect hydraulics through changes in anatomy (i.e., wood density, proportions of fiber, and parenchyma) (Lourenço et al., 2022), in addition to water table depth, which affects water availability to plants within the same precipitation regime. Accounting for WTD might decrease the predictive capacity of MCWD because, in places with lower precipitation and high VPD, valleys still have more available water via groundwater

than the plateaus within the same region, compromising the simple correlation of MCWD with hydraulic traits. We found that shallow WTDs, which provide easier root access to water (Fan et al., 2017), were consistently associated with decreased embolism resistance (Figure 1a,d,g). These patterns have been previously shown for the Amazon only at local scales (Fontes et al., 2020; Garcia, Hu, et al., 2021; Oliveira et al., 2019). Here, we are able, for the first time, to extend these results to larger scales and across different regions of the Amazon basin, showing that water table depth is a stronger driver of embolism resistance of Amazon trees than climatic water deficit. This has important implications for the future of forests in wetlands, valleys and other shallow water table sites (50% of the Amazonian area (Costa et al., 2023)), which can function as hydrological refugia due to groundwater supply in moderate droughts, but are in danger of a collapse in strong droughts due to vulnerable hydraulic systems (Costa et al., 2023; Flores et al., 2017).

Our results show that fertility and its interaction with precipitation affect a site's average tree hydraulic strategy and specifically affect different phases of the embolism process (i.e., P12, P50 and P88). This result helps to explain why the impact of climate water deficit is less important than fertility for predicting hydraulic responses along the environmental gradients of the Amazon—assessing the environmental effects throughout the sequential phases of the embolism process allowed for detecting responses that are expected to limit severe drought damage to plants lacking resistant hydraulic systems. The divergent response of P12 and P50 under the same precipitation deficit caused by fertility was surprising (Figure 1c,f). The expectation is that high MCWD, on average, selects conservative trees that can tolerate high water potentials with high embolism resistance (Tavares et al., 2023). However, our results show that high MCWD combined with high fertility drove low embolism resistance. These effects may arise because earlier phases of embolism formation are potentially at levels where stomatal regulation can strongly mitigate further embolism, for example, by preventing the development of higher xylem pressures. Plants are expected to undergo stomatal closure before reaching sufficiently low water potentials (more negative) to prevent wilting and substantial declines in stem hydraulic conductivity (i.e., ≥50% decline). The effect of soil fertility on hydraulics may start at the leaf level since increasing exchangeable cation concentrations would improve stomatal regulation through osmoregulation (Wang et al., 2016). Specifically, potassium is an enzyme cofactor, an osmolyte and an electrolyte in cell membranes. Thus, increased potassium concentration could improve the efficiency of stomatal control (Liu et al., 2006) at the beginning of the cavitation process, which in turn could provide a sizable hydraulic safety margin and protect the hydraulic system from increasing embolism. High nutrient levels offer a rescue pathway to drought protection through stomatal regulation. This strategy works well in short droughts, such as those experienced by Amazonian forests in 2015 (Garcia, Ferreira, et al., 2021). However, this route is probably insufficient to prevent hydraulic failure under prolonged or more intense droughts. Due to the potential differences in plant nutrient functions, disentangling the role of each nutrient on plant hydraulics will require specific experiments to investigate and confirm such effects. Thus, our results indicate that higher MCWD is indeed associated with the construction of safer xylem tissues, but only when combined with low soil fertility, critically expanding the current knowledge (Tavares et al., 2023).

The effect of soil fertility on tree hydraulic responses has not been tested before at the large scale of the Amazon basin. However, this hypothesis has been raised recently based on empirical data (Oliveira et al., 2021). The hypothesis assumes that the 'fast-slow' plant economics spectrum should hold across all organs and resources, as previously proposed (Reich, 2014). In that case, the logic is straightforward: adjustments to nutrient and water levels might be part of the same evolutionary strategy, as they require adaptive traits operating in the same direction. In resource-rich conditions, these traits promote high water conductivity to supply the leaves and high nutrient acquisition and consumption rates, resulting in fast growth rates and, thus, a reduction in the residence time of these resources in the plant. On the opposite side, when there is a low resource supply, investments in strong tissues to protect the hard-won nutrients help create a safe hydraulic system and reduce the water needed to supply the slow growth. Our results partially confirm this hypothesis, as we detect a convergence of hydraulic resistance values at low fertility levels (Figure 1e,h), but at the same time, we show that high fertility can drive a much more varied range of embolism resistance (Figures 1c,f and 3). High variability in more productive sites may be an inherent consequence of their faster dynamics (Lewis et al., 2004), which creates more light gaps and thus high niche diversity, sustaining alternative plant designs with different solutions to local conditions and thus supporting coexistence of a more diverse local community (Dias et al., 2020; Marks & Lechowicz, 2006a, 2006b). At the same time, we show that a large fraction of individuals on fertile soils has unsafe hydraulic traits, so despite the variation, those areas are still predicted to be more vulnerable to drought based on the traits examined here. Interestingly, Tavares et al. (2023) showed that the southern band of Amazonia has the most vulnerable plant community. The explanation they provided for this was that this region is the driest of the Amazon and also the one that has faced the most significant recent climatic changes. Our results are consistent with that study. However, we bring an additional explanation: the dry climate combined with intermediate-to-high soil fertility selects plants with a more vulnerable hydraulic system that translates into a lower hydraulic safety margin. For example, their comparison of two of their sites is illustrative of that: the NVX site, with a very long dry season, but intermediate fertility soils has less negative P50 than the TAP site, which has a less pronounced dry season but very infertile soils. With this, we broaden the understanding of why hydraulic vulnerability drivers go beyond annual precipitation.

This study is the first empirical large-scale demonstration that hydraulic traits can be selected according to some of the same principles applying to the carbon economy traits, that is, by gradients of resource levels, where fertility plays a central role. Consequently, any attempt to determine ecosystem susceptibility to climate change impacts based on hydraulic traits must be based on an integrated

assessment of what environmental factors are driving the mechanisms. Nevertheless, since the trait filtering is not perfectly matched to the resource gradients, the modelling of ecosystem vulnerability must go beyond findings based only on economic traits (Joswig et al., 2022) or theoretical grounds (Joswig et al., 2022; Oliveira et al., 2021). A comprehensive understanding of ecosystem vulnerability to drought should consider whole-tree traits, including root, stem and leaf.

The spatial projection of our results to the whole Amazon basin indicates a large southern band as the most hydraulically vulnerable region, primarily due to fertile soils, and this is also the region with the lowest uncertainties of the model projection (Figure S8). Current knowledge about tree mortality in the Amazon suggests that species-level growth rate is the most critical predictor of tree death, with faster-growing species at higher risk (Esquivel-Muelbert et al., 2020). We found that the embolism resistance values derived from the mapping projection of our models over the Amazon basin were related to the independent data on average mortality rates (Esquivel-Muelbert et al., 2020). Ecosystem-level studies show that forests in fertile soils have higher mortality rates on average (Quesada et al., 2012). These high mortality rates emerge from the short life cycles of fast-growing plants irrespective of climate, but droughts may exacerbate the trend, creating an excess of death. However, alternative strategies to cope with drought can be found to be linked to environmental buffers or plant strategies, as discussed above. Alternatively, plants growing in fertile soils may grow faster (Malhi et al., 2015) because they develop a less embolism-resistant hydraulic system, as evidenced by this study, which would help explain the excess of death caused by drought if there is some. A definitive conclusion requires an analysis of tree mortality caused only by drought.

Additionally, the hydrological environment could protect plants from drought-induced mortality—trees growing over terrains with easy access to the groundwater (Sousa et al., 2020) could survive with intermediate-vulnerable hydraulic systems, as we find in this study. However, plants may develop safer hydraulic or deep root systems to access water when the hydrological environment does not provide protection, such as when the water table is deep. The presence of these strategies to deal with drought (ample water supply to roots or efficient stomatal regulation) increases the resilience of the forest under current environmental conditions. Regardless, under the intensification of droughts expected for the future, we predict from our results that trees growing in forests with high soil fertility—which are the most productive in the Amazon—will be more likely to reach a threshold where leaf and root strategies will eventually fail. Given that the next level of plant response—at the hydraulic system itself (here represented by P50 and P88), was found to be the most vulnerable in soils with more phosphorus, these forests can be expected to be in great danger. Forests over shallow water tables are next in the vulnerability line if droughts are intense enough to lower water table depths beyond the reach of roots, especially when shallow WTD is combined with fertile soils.

Some limitations of this study include the need for further research to determine the relationship between the estimated hydraulic traits and mortality caused exclusively by drought, as there is currently a lack of drought-induced mortality data covering the broad environmental gradients of the Amazon. Second, the study does not cover the entire precipitation spectrum of the Amazon (although the sampled range—80 to 337 mm MCWD was extensive in comparison with the total range of 0 to 489 mm MCWD, see details in Figure S4), which could potentially affect the relative contribution of precipitation to the patterns observed. Third, the study has focused on the abundant species of each site, and as such, conveys a picture of the dominant traits, which are expected to affect ecosystem-level responses to drought. However, these patterns may not represent well the less abundant species that contribute to the large species diversity of tropical forests, and these still need to be investigated. Last, more research is needed to integrate the hydraulic traits examined in this study with a broader suite of traits to better understand tree survival strategies.

In conclusion, this study proposes a way forward in understanding tree vulnerability to droughts in the Amazon. The geography of hydraulic traits provided in this study is a starting point to indicate where, spatially, drought could most affect trees, helping to direct investments to collect a more comprehensive ecophysiological data set in places with high hydraulic variation.

4 | MATERIALS AND METHODS

4.1 | Study sites and sampling design

We performed hydraulic measurements at four sites in the Amazon region. We cover three key fertility regions across the Amazon basin, as identified by Quesada et al. (2009): Central Amazon, the Western peripheral area and the Brazilian Shield. We used a nested design covering all the combinations of high and low climatic water deficit, high and low soil fertility and high and low water table depths. The four sites represent the combinations of climate and soil fertility. Within each of those sites, topographic positions with low- and high-water-table depths were sampled (Figure S1) and consequently covered a high functional variation in hydraulic traits.

Ducke Reserve (AM-DUCK) was our high precipitation/low water deficit and low fertility site, covering 10,000 ha in the central Amazon region (2° 55′ 47.80″ S; 59° 58′ 30.34″ W). The total annual precipitation is 2258 mm, and the average maximum climatological water deficit (MCWD) is −80 mm (from Tropical Rainfall Measuring Mission—TRMM https://disc2.gesdisc.eosdis.nasa.gov/data/TRMM_L3/TRMM_3B43.7/). Climate data used in the description of sites were based on monthly averages from 2000 to 2021. The soils are mainly derived from rocks and sediments from the middle Tertiary and thus have likely experienced more or less continuous weathering for more than 20 million years (Quesada et al., 2009), resulting in low nutrient concentration (average of 0.16 cmol/kg of exchangeable bases). There is a continuum of soil texture change from clay rich in the plateaus to sandy in the valleys. The predominant vegetation type is dense lowland *terra-firme* rainforest.

Uatumã Biological Reserve (AM-REBI) was our high precipitation/low water deficit and high soil fertility site, covering 1 million ha in the central Amazon region (1° 48′ 00″ S, 59° 15′ 00″ W). The average annual rainfall is 2405 mm, with an average MCWD of −96 mm (from TRMM). The entire reserve consists of rolling hills, with as much as a 100 m difference in height from low to high areas. It lies on the boundary between the sedimentary Palaeozoic Trombetas formation and an igneous/volcanic Precambrian formation (Irion, 1978). Soils form a gradient from poor latosols to richer soils derived from outcrops of igneous Precambrian rocks of the Guiana Shield. Specifically, we selected only plots with high fertility in this region (at least 3.5 cmol/kg of exchangeable bases). The predominant vegetation types are primary lowland and submontane-dense *terra-firme* rainforest.

Experimental farm Catuaba (AC-CATU) was our low precipitation/high water deficit and high soil fertility site, covering 2111 ha in the Western peripheral area (10° 04′ S e 67° 37′ W). The average annual precipitation is 1956 mm with an average MCWD of −228 mm (from TRMM). The soils are predominantly oxisols and argisoils. Due to its proximity to the Andes, where soil surface erosion exposes parent material, the region maintains high fertility (average of 1.8 cmol/kg of exchangeable bases). Topography is gently undulating. The predominant primary vegetation types are dense lowland *terra-firme* rainforests and open forests with a large abundance of bamboo and palms (Silveira et al., 2008).

The site with low precipitation/high water deficit and low soil fertility (MT-COTR) was at São Nicolau farm belonging to ONF Brasil, in the Brazilian shield region (9° 51′ 25″ S and 58° 14′ 55″ W). The average annual precipitation is 1906 mm with an average MCWD of −337 mm (from TRMM). Soils are derived from igneous and metamorphic rocks of the Precambrian Brazilian shield. These are the oldest surfaces exposed in South America, with their maximum geological age ranging from 1.5 to 3.6 billion years. Specifically, we selected sites with low fertility (average of 0.85 cmol/kg of exchangeable bases). Topography is gently undulating. The predominant vegetation type is dense and open submontane rainforest.

4.2 | Environmental measurements

In order to represent the local hydrological environments, we used the water table depth (WTD) layer produced by Fan et al. (2013) with a spatial resolution of ~270 m. To evaluate the effect of precipitation deficit on hydraulic traits, we used the maximum climatological water deficit (MCWD) calculated as the maximum value of the accumulated water deficit for each pixel within the year (Aragão et al., 2007). Precipitation was obtained from the 2000 to 2018 time series of the Tropical Rainfall Measuring Mission. To include the accumulated deficit of the entire low precipitation period, we defined our 'hydrological year' as the 12-month period running from May to April. Evapotranspiration (ET) was fixed at 100 mm per month, a value derived from the mean evapotranspiration measured at different locations and stations in the Amazon (von Randow et al., 2004). The vapour pressure deficit was another relevant determinant of plant water relations, but it had a high correlation with MCWD ($R=0.8$, $p<0.001$) and thus was not included in the models. Soil fertility depends on many nutrients, but in the Amazon, phosphorus tends to be limited and considered key to forest productivity (Quesada et al., 2009). Due to the diversity of soil formations in the Amazon, originating from varied geological and geomorphological contexts and ages, we considered two metrics to represent soil fertility: the concentration of exchangeable cations (Ca + Mg + K measured in cmol/kg) and phosphorus (mg/kg). Generally, phosphorus and cation concentrations are higher in younger soils, such as those derived from the Andes, while older soils in the Brazilian and Guiana Shields are poor in phosphorus. However, the central Amazon has several areas with soils derived from igneous Precambrian outcrops with high cation concentrations but low phosphorus, leading to an overall low correlation between cation and phosphorus concentrations in our sampled plots (Figure S2). The soil fertility data were directly measured for each plot at the local scale. Soil texture is also a determinant of soil water availability, but fractions of sand or clay were highly correlated with the water table depth in our dataset (clay, $R^2=0.57$; sand $R^2=-0.40$, $p<0.001$ in both cases) and thus not included in the models.

4.3 | Vulnerability curves

Measurements were taken in 2016 in one site (AM-DUCK) and in 2019 in three other sites, sampling 165 individuals of 64 species (See details in Table S1). In this study, we want to understand forest vulnerability to drought impacts at the ecosystem level; accordingly, we are focusing on the dominant species. We selected the dominant species of each climate–soil–WTD combination based on the rankings of basal area and stem number. Despite a low sample size for the Amazonian scale, we cover a wide range of hydraulic traits considering tropical forests (Figure S3) and a large range of environmental conditions (Figure S4). The collection was performed in a typical year during the wet season. To standardize the height of the sampled branch in relation to the total height of the tree, branches were collected from the middle portion of the crown using a pruner. To ensure that vessels were closed, we collected 70- to 200-cm-long branches (Garcia, Hu, et al., 2021) and for the distribution of maximum vessel lengths. All collections were made at pre-dawn. Once the branches were collected, they were wrapped in a moist paper towel and placed into a dark plastic bag. The samples were returned to the lab within 1–3 h of branch collection.

In the lab, we used the pneumatic method (Pereira et al., 2016; Zhang et al., 2018) to obtain per cent loss of conductivity (PLC) curves in relation to the declining water potential (Ψ_x). We took branch water potential measurements at full hydration using a pressure chamber (PMS, Pressure Chamber Instrument, Oregon, USA), followed by air discharge measurements. We used the benchtop dehydration method to decrease the branch water potential values (Sperry & Saliendra, 1994), drying the branches while measuring

Ψ_x until full dehydration. We also measured the corresponding air discharge values. Measurements were made on two branches per individual tree. Before each measurement, we sealed our branches in a dark plastic bag for 40–60 min to equilibrate the xylem water potential. We calculated each branch's per cent loss conductivity (PLC), considering the minimum and maximum values. We pooled the data from the two branches replicated from the same tree to calculate 12%, 50% and 88% loss of conductivity (i.e., P12, P50 and P88). We fitted a line using a nonlinear two-parameter Weibull equation (Equation 1).

$$PLC = 1 - e^{-(\Psi_x/b)^K} \quad (1)$$

where Ψ_x is the xylem water potential, b the scale parameter and K the shape parameters to be estimated. The coefficients were estimated using nonlinear least-squares fitting using the *optimx* package in R (R Core Team, 2020).

We discarded some unreliable or overly noisy individual vulnerability curve measurements, ending with 109 individuals (see the individual curves in Figure S5).

4.4 | Statistical analysis

To answer the first question—How do climatic water deficit, soil fertility and water table depth affect P12, P50 and P88 across the Amazon? We evaluate the effects of standardized soil phosphorus content (or exchangeable cations concentration), MCWD and WTD on plant hydraulic resistance with generalized linear models (GLM). Alternative models, including random factors for species and sites, were also tested to check if phylogenetic or spatial autocorrelation affected the results (Tables S3–S6). Data points on those analyses were the individual-level values of hydraulic traits. Data distributions were selected to the best fit in each analysis; we used gamma distributions for P50 and P88 and Gaussian distributions for P12. We used unsupervised model selection [dredge function, MuMIn package (Bartón, 2016)]. We established a correlation rule excluding fixed-effects variable pairs whose correlation was >0.4 (pairwise correlations in Figure S6). We have allowed all the possible interactions among the three predictor variables. To identify the best model set, we applied the Akaike information criterion, with a correction for small sample sizes (AICc) to avoid the risk of overfitting. AICc applies a bias-corrected form, which adds a penalty on the number of parameters. All models within two units of the model with the lowest AICc were considered as having strong support, and the model with the lowest AICc value was assigned as the 'best model' (Burnham & Anderson, 2002). We used the *visreg* package in R to plot the partial effects of multiple regressions (Breheny & Burchett, 2017). We used WTD and MCWD values on the positive scale, representing the increasing depth of water tables and increasing climatological water deficit. To answer our second question—Is there a difference in the predictive power of the environmental variables for P12, P50 and P88? We computed the relative weight of each predictor. This was achieved by summing model weights across all the models in the full set in which the respective predictor occurred. To test the phylogenetic signal, we estimated Blomberg's K with the function phylosignal of the R package 'picante' (Kembel et al., 2010). Blomberg's K is a measure of the strength of phylogenetic signal in a dataset. It is calculated as the ratio of the mean squared error of the tip data (MSE0), which is measured from the phylogenetically corrected mean, to the mean squared error (MSE) based on the variance–covariance matrix derived from the phylogeny under the assumption of Brownian motion evolution. When trait values are well predicted by the phylogeny, MSE is small, resulting in a large MSE0/MSE ratio (Blomberg et al., 2003). To build our phylogeny, we used V.PhyloMaker package (Jin & Qian, 2019, 2022).

In order to generate predictions of the geographical distribution of hydraulic traits, we modelled the hydraulic tree responses in our sites using environmental predictors derived from basin-scale layers. Then, we upscaled the predicted hydraulic values to maps of the Amazon basin. We used WTD from Fan et al. (2013), and MCWD from TRMM, as described in the environmental measurements section. In the absence of a spatial layer for phosphorus, we used the distribution model of exchangeable cation concentration across Amazonia (Zuquim et al., 2019) as our soil fertility layer. We used a 1 km grid in each layer to obtain the environmental values for the basin-scale model. We used the coefficients of our best model (not including species effects since this would require knowledge of the species composition for all pixels) for the upscaling mapping (see Table S2). Then, we produced the geographical distribution of P12, P50 and P88. To determine the agreement of models using local versus basin modelled soil fertility data, we compared models considering the concentration of exchangeable cations directly measured at the local scale of each plot against those using the values derived from the basin-scale map of Zuquim et al. (2019) (Table S2). To investigate the utility of our hydraulic resistance maps as a resource to predict mortality across the basin, we extracted the estimated values of P12, P50 and P88 for the pixels where there were mortality rate data from Esquivel-Muelbert et al. (2020). We related embolism resistance to mortality rates with simple regressions. We used this dataset for mortality because, so far, it is the largest mortality database for Amazon (131 sites).

To estimate the uncertainties linked to the predictions of P12, P50 and P88, we employed geospatial mapping techniques based on the standard error from our GLM model. Utilizing the *ggplot2* package, raster maps were generated to visualize the standard error categories associated with each variable. We established four distinct uncertainty categories based on the range of standard errors: for P12 and P50, low (0–1.2 MPa), medium (1.2–1.8 MPa) and high (>1.8 MPa), and P88 low (0–1.55 MPa), medium (1.55–2.06 MPa) and high (>2.06 MPa) (Figure S8), enabling a visual assessment of the reliability of predictions across the study area. The threshold for defining the categories was based on 25%, 50% and 75% quantiles.

Lastly, we looked at the frequency distributions of estimated hydraulic resistance values along the fertility and water table depth categories, using the median as a reference. The values above 1.21

cmol/kg were classified as high fertility, with the deep water table classified as >5 m.

All analyses were performed in R (R Core Team, 2020). The GLM analysis used the glm package (Hastie & Pregibon, 2017), and maps were produced with the raster package (Hijmans et al., 2013).

AUTHOR CONTRIBUTIONS

Maquelle N. Garcia, Flávia R. C. Costa, Tomas F. Domingues and Rafael S. Oliveira designed the research. Maquelle N. Garcia collected the data. Maquelle N. Garcia analysed the data. Maquelle N. Garcia and Flávia R. C. Costa interpreted the analysis and results. Maquelle N. Garcia wrote the first draft and Flávia R. C. Costa, Tomas F. Domingues and Rafael S. Oliveira contributed writing to the manuscript.

ACKNOWLEDGEMENTS

We thank the National Institute of Amazon Research (INPA) for logistic support; the Brazilian Program for Biodiversity Research (PPBio) and the Brazilian LTER (PELD), which established and monitored plots and species used here; the US Agency for International Development (USAID) and the partnership for enhanced engagement in research programme (PEER) for a research scholarship; the Coordination for Improvement of Higher Level Personnel (CAPES) for a scholarship and partial funding—Finance Code 001; the Federal University of Mato Grosso (UFMT) including professor Domingos Rodrigues and his team; Federal University of Acre (UFAC) including professor Marcos Silveira and his team; The Chico Mendes Institute (ICMBio) and their team for all logistical support and additional information to facilitate sampling; for invaluable help with field and lab work: João Sousa, Davieliton Mesquita, Mara Paneghel, Carla Lang, Ivan Santos, Jennifer Miranda, Moisés Stofel, Jefferson Sousa and Gleisson Viana; Paulo Bittencourt, Mauro Brum and Luciano Pereira for discussions about the pneumatics method; Shuli Chen for discussions on spatial projections of models; and Charles Southwick for the English review.

FUNDING INFORMATION

This work was funded via the PEER programme (grant agreement AID-OAA-A-11-00012) to TFD and RSO, and CNPq/PELD grants #441282/2016-4, 403764/2012-2 and 558244/2009-2 to FRCC and FAPEAM N.009/2021—PROFIX-RH Nº 01.02.016301.00411/2022-52 to MNG.

CONFLICT OF INTEREST STATEMENT

The authors declare that they have no competing interests.

DATA AVAILABILITY STATEMENT

The data used in this study are available at the following link: https://search.dataone.org/view/PPBioAmOc.688.2.

ORCID

Maquelle N. Garcia https://orcid.org/0000-0003-2533-398X

REFERENCES

Anderegg, W. R. L., Klein, T., Bartlett, M., Sack, L., Pellegrini, A. F. A., Choat, B., & Jansen, S. (2016). Meta-analysis reveals that hydraulic traits explain cross-species patterns of drought-induced tree mortality across the globe. *Proceedings of the National Academy of Sciences of the United States of America*, *113*, 5024–5029.

Aragão, L. E. O. C., Malhi, Y., Roman-Cuesta, R. M., Saatchi, S., Anderson, L. O., & Shimabukuro, Y. E. (2007). Spatial patterns and fire response of recent Amazonian droughts. *Geophysical Research Letters*, *34*, 948.

Baraloto, C., Timothy Paine, C. E., Poorter, L., Beauchene, J., Bonal, D., Domenach, A.-M., Hérault, B., Patiño, S., Roggy, J.-C., & Chave, J. (2010). Decoupled leaf and stem economics in rain forest trees. *Ecology Letters*, *13*, 1338–1347.

Bartón, K. (2016). *Multi-model inference*. R package version 3.3.0.

Blomberg, S. P., Garland, T., Jr., & Ives, A. R. (2003). Testing for phylogenetic signal in comparative data: Behavioral traits are more labile. *Evolution*, *57*, 717–745.

Breheny, P., & Burchett, W. (2017). Visualization of regression models using visreg. *The R Journal*, *9*, 56–71. https://journal.r-project.org/archive/2017/RJ-2017-046/

Brodribb, T. J., Powers, J., Cochard, H., & Choat, B. (2020). Hanging by a thread? Forests and drought. *Science*, *368*, 261–266.

Brum, M., Vadeboncoeur, M. A., Ivanov, V., Asbjornsen, H., Saleska, S., Alves, L. F., Penha, D., Dias, J. D., Aragão, L. E. O. C., Barros, F., Bittencourt, P., Pereira, L., & Oliveira, R. S. (2019). Hydrological niche segregation defines forest structure and drought tolerance strategies in a seasonal Amazon forest. *The Journal of Ecology*, *107*, 318–333.

Burnham, K. P., & Anderson, D. R. (2002). A practical information-theoretic approach. *Model Selection and Multimodel Inference*, *2*, 49–86.

Choat, B., Jansen, S., Brodribb, T. J., Cochard, H., Delzon, S., Bhaskar, R., Bucci, S. J., Feild, T. S., Gleason, S. M., Hacke, U. G., Jacobsen, A. L., Lens, F., Maherali, H., Martínez-Vilalta, J., Mayr, S., Mencuccini, M., Mitchell, P. J., Nardini, A., Pittermann, J., … Zanne, A. E. (2012). Global convergence in the vulnerability of forests to drought. *Nature*, *491*, 752–755.

Costa, F. R. C., Schietti, J., Stark, S. C., & Smith, M. N. (2023). The other side of tropical forest drought: Do shallow water table regions of Amazonia act as large-scale hydrological refugia from drought? *The New Phytologist*, *237*, 714–733.

Dias, A. T. C., Rosado, B. H. P., De Bello, F., Pistón, N., & De Mattos, E. A. (2020). Alternative plant designs: Consequences for community assembly and ecosystem functioning. *Annals of Botany*, *125*, 391–398.

Esquivel-Muelbert, A., Phillips, O. L., Brienen, R. J. W., Fauset, S., Sullivan, M. J. P., Baker, T. R., Chao, K.-J., Feldpausch, T. R., Gloor, E., Higuchi, N., Houwing-Duistermaat, J., Lloyd, J., Liu, H., Malhi, Y., Marimon, B., Marimon Junior, B. H., Monteagudo-Mendoza, A., Poorter, L., Silveira, M., … Galbraith, D. (2020). Tree mode of death and mortality risk factors across Amazon forests. *Nature Communications*, *11*, 5515.

Fan, Y., Li, H., & Miguez-Macho, G. (2013). Global patterns of groundwater table depth. *Science*, *339*, 940–943.

Fan, Y., Miguez-Macho, G., Jobbágy, E. G., Jackson, R. B., & Otero-Casal, C. (2017). Hydrologic regulation of plant rooting depth. *Proceedings of the National Academy of Sciences of the United States of America*, *114*, 10572–10577.

Flores, B. M., Holmgren, M., Xu, C., van Nes, E. H., Jakovac, C. C., Mesquita, R. C. G., & Scheffer, M. (2017). Reply to Schöngart et al.: Forest resilience variation across Amazonian floodplains. *Proceedings of the National Academy of Sciences of the United States of America*, *114*, E8552–E8554.

Fontes, C. G., Fine, P. V. A., Wittmann, F., Bittencourt, P. R. L., Piedade, M. T. F., Higuchi, N., Chambers, J. Q., & Dawson, T. E. (2020). Convergent evolution of tree hydraulic traits in Amazonian habitats: Implications for community assemblage and vulnerability to drought. *The New Phytologist*, *228*, 106–120.

Garcia, M. N., Ferreira, M. J., Ivanov, V., Dos Santos, V. A. H. F., Ceron, J. V., Guedes, A. V., Saleska, S. R., & Oliveira, R. S. (2021). Importance of hydraulic strategy trade-offs in structuring response of canopy trees to extreme drought in Central Amazon. *Oecologia*, *197*, 13–24.

Garcia, M. N., Hu, J., Domingues, T. F., Groenendijk, P., Oliveira, R. S., & Costa, F. R. C. (2021). Local hydrological gradients structure high intraspecific variability in plant hydraulic traits in two dominant central Amazonian tree species. *Journal of Experimental Botany*, *73*, 939–952.

Gleason, S. M., Westoby, M., Jansen, S., Choat, B., Hacke, U. G., Pratt, R. B., Bhaskar, R., Brodribb, T. J., Bucci, S. J., Cao, K.-F., Cochard, H., Delzon, S., Domec, J.-C., Fan, Z.-X., Feild, T. S., Jacobsen, A. L., Johnson, D. M., Lens, F., Maherali, H., … Zanne, A. E. (2016). Weak tradeoff between xylem safety and xylem-specific hydraulic efficiency across the world's woody plant species. *The New Phytologist*, *209*, 123–136.

Grime, J. P. (1977). Evidence for the existence of three primary strategies in plants and its relevance to ecological and evolutionary theory. *The American Naturalist*, *111*, 1169–1194.

Guillemot, J., Martin-StPaul, N. K., Bulascoschi, L., Poorter, L., Morin, X., Pinho, B. X., le Maire, G., Bittencourt, P., Oliveira, R. S., Bongers, F., Brouwer, R., Pereira, L., Melo, G. A. G., Boonman, C. C. F., Brown, K. A., Cerabolini, B. E. L., Niinemets, Ü., Onoda, Y., Schneider, J. V., … Brancalion, P. H. S. (2022). Small and slow is safe: On the drought tolerance of tropical tree species. *Global Change Biology*, *28*(8), 2622–2638.

Hastie, T. J., & Pregibon, D. (2017). Generalized linear models. In *Statistical models in S* (pp. 195–247). Routledge.

Hijmans, R. J., van Etten, J., Mattiuzzi, M., Sumner, M., Greenberg, J. A., Lamigueiro, O. P., Bevan, A., Racine, E. B. & Shortridge, A. (2013). Raster package in R. Version. https://mirrors.sjtug.sjtu.edu.cn/cran/web/packages/raster/raster.pdf

Irion, G. (1978). Soil infertility in the Amazonian rain forest. *Die Naturwissenschaften*, *65*, 515–519.

Jin, Y., & Qian, H. (2019). V.PhyloMaker: An R package that can generate very large phylogenies for vascular plants. *Ecography*, *42*, 1353–1359.

Jin, Y., & Qian, H. (2022). V.PhyloMaker2: An updated and enlarged R package that can generate very large phylogenies for vascular plants. *Plant Diversity*, *44*, 335–339.

Joswig, J. S., Wirth, C., Schuman, M. C., Kattge, J., Reu, B., Wright, I. J., Sippel, S. D., Rüger, N., Richter, R., Schaepman, M. E., van Bodegom, P. M., Cornelissen, J. H. C., Díaz, S., Hattingh, W. N., Kramer, K., Lens, F., Niinemets, Ü., Reich, P. B., Reichstein, M., … Mahecha, M. D. (2022). Climatic and soil factors explain the two-dimensional spectrum of global plant trait variation. *Nature Ecology & Evolution*, *6*, 36–50.

Kembel, S. W., Cowan, P. D., Helmus, M. R., Cornwell, W. K., Morlon, H., Ackerly, D. D., Blomberg, S. P., & Webb, C. O. (2010). Picante: R tools for integrating phylogenies and ecology. *Bioinformatics*, *26*, 1463–1464.

Lewis, S. L., Phillips, O. L., Baker, T. R., Lloyd, J., Malhi, Y., Almeida, S., Higuchi, N., Laurance, W. F., Neill, D. A., Silva, J. N. M., Terborgh, J., Lezama, A. T., Martínez, R. V., Brown, S., Chave, J., Kuebler, C., Vargas, P. N., & Vinceti, B. (2004). Concerted changes in tropical forest structure and dynamics: Evidence from 50 south American long-term plots. *Philosophical Transactions of the Royal Society of London. Series B, Biological Sciences*, *359*, 421–436.

Liu, H., Ye, Q., Gleason, S. M., He, P., & Yin, D. (2021). Weak tradeoff between xylem hydraulic efficiency and safety: Climatic seasonality matters. *The New Phytologist*, *229*, 1440–1452.

Liu, H.-Y., Sun, W.-N., Su, W.-A., & Tang, Z.-C. (2006). Co-regulation of water channels and potassium channels in rice. *Physiologia Plantarum*, *128*, 58–69.

Lourenço, J., de Lima Bittencourt, P. R., Enquist, B. J., Milanez, C. R. D., von Arx, G., Morino, K., Thomaz, L. D., & Rowland, L. (2022). Fiber-parenchyma trade-off underlies changes in tropical forest structure and xylem architecture across a soil water gradient. *bioRxiv*, 2022.01.13.476164.

Malhi, Y., Doughty, C. E., Goldsmith, G. R., Metcalfe, D. B., Girardin, C. A. J., Marthews, T. R., Del Aguila-Pasquel, J., Aragão, L. E. O. C., Araujo-Murakami, A., Brando, P., da Costa, A. C. L., Silva-Espejo, J. E., Farfán Amézquita, F., Galbraith, D. R., Quesada, C. A., Rocha, W., Salinas-Revilla, N., Silvério, D., Meir, P., & Phillips, O. L. (2015). The linkages between photosynthesis, productivity, growth and biomass in lowland Amazonian forests. *Global Change Biology*, *21*, 2283–2295.

Maréchaux, I., Bartlett, M. K., Sack, L., Baraloto, C., Engel, J., Joetzjer, E., & Chave, J. (2015). Drought tolerance as predicted by leaf water potential at turgor loss point varies strongly across species within an Amazonian forest. *Functional Ecology*, *29*, 1268–1277.

Marks, C. O., & Lechowicz, M. J. (2006a). A holistic tree seedling model for the investigation of functional trait diversity. *Ecological Modelling*, *193*, 141–181.

Marks, C. O., & Lechowicz, M. J. (2006b). Alternative designs and the evolution of functional diversity. *The American Naturalist*, *167*, 55–66.

McDowell, N., Allen, C. D., Anderson-Teixeira, K., Brando, P., Brienen, R., Chambers, J., Christoffersen, B., Davies, S., Doughty, C., Duque, A., Espirito-Santo, F., Fisher, R., Fontes, C. G., Galbraith, D., Goodsman, D., Grossiord, C., Hartmann, H., Holm, J., Johnson, D. J., … Xu, X. (2018). Drivers and mechanisms of tree mortality in moist tropical forests. *The New Phytologist*, *219*, 851–869.

McDowell, N., Pockman, W. T., Allen, C. D., Breshears, D. D., Cobb, N., Kolb, T., Plaut, J., Sperry, J., West, A., Williams, D. G., & Yepez, E. A. (2008). Mechanisms of plant survival and mortality during drought: Why do some plants survive while others succumb to drought? *The New Phytologist*, *178*, 719–739.

McDowell, N. G. (2011). Mechanisms linking drought, hydraulics, carbon metabolism, and vegetation mortality. *Plant Physiology*, *155*, 1051–1059.

Oliveira, R. S., Costa, F. R. C., van Baalen, E., de Jonge, A., Bittencourt, P. R., Almanza, Y., Barros, F. D. V., Cordoba, E. C., Fagundes, M. V., Garcia, S., Guimaraes, Z. T. M., Hertel, M., Schietti, J., Rodrigues-Souza, J., & Poorter, L. (2019). Embolism resistance drives the distribution of Amazonian rainforest tree species along hydro-topographic gradients. *The New Phytologist*, *221*, 1457–1465.

Oliveira, R. S., Eller, C. B., De Barros, F. V., Hirota, M., Brum, M., & Bittencourt, P. (2021). Linking plant hydraulics and the fast–slow continuum to understand resilience to drought in tropical ecosystems. *The New Phytologist*, *230*, 904–923.

Pereira, L., Bittencourt, P. R. L., Oliveira, R. S., Junior, M. B. M., Barros, F. V., Ribeiro, R. V., & Mazzafera, P. (2016). Plant pneumatics: Stem air flow is related to embolism—New perspectives on methods in plant hydraulics. *The New Phytologist*, *211*, 357–370.

Phillips, O. L., Aragão, L. E. O. C., Lewis, S. L., Fisher, J. B., Lloyd, J., López-González, G., Malhi, Y., Monteagudo, A., Peacock, J., Quesada, C. A., van der Heijden, G., Almeida, S., Amaral, I., Arroyo, L., Aymard, G., Baker, T. R., Bánki, O., Blanc, L., Bonal, D., … Torres-Lezama, A. (2009). Drought sensitivity of the Amazon rainforest. *Science*, *323*, 1344–1347.

Powers, J. S., Vargas, G. G., Brodribb, T. J., Schwartz, N. B., Pérez-Aviles, D., Smith-Martin, C. M., Becknell, J. M., Aureli, F., Blanco, R., Calderón-Morales, E., Calvo-Alvarado, J. C., Calvo-Obando, A. J., Chavarría, M. M., Carvajal-Vanegas, D., Jiménez-Rodríguez, C. D., Murillo Chacon, E., Schaffner, C. M., Werden, L. K., Xu, X., & Medvigy, D. (2020). A catastrophic tropical drought kills

hydraulically vulnerable tree species. *Global Change Biology*, *26*, 3122–3133.

Quesada, C. A., Lloyd, J., Anderson, L. O., Fyllas, N. M., Schwarz, M., & Czimczik, C. I. (2009). Soils of Amazonia with particular reference to the rainfor sites. *Biogeosciences Discussions*, *6*, 3851–3921.

Quesada, C. A., Phillips, O. L., Schwarz, M., Czimczik, C. I., Baker, T. R., Patiño, S., Fyllas, N. M., Hodnett, M. G., Herrera, R., Almeida, S., Alvarez Dávila, E., Arneth, A., Arroyo, L., Chao, K. J., Dezzeo, N., Erwin, T., di Fiore, A., Higuchi, N., Honorio Coronado, E., … Lloyd, J. (2012). Basin-wide variations in Amazon forest structure and function are mediated by both soils and climate. *Biogeosciences*, *9*, 2203–2246.

R Core Team. (2020). *R: A language and environment for statistical computing*. R Foundation for Statistical Computing https://www.r-project.org/

Reich, P. B. (2014). The world-wide "fast-slow" plant economics spectrum: A traits manifesto. *The Journal of Ecology*, *102*, 275–301.

Rowland, L., da Costa, A. C. L., Galbraith, D. R., Oliveira, R. S., Binks, O. J., Oliveira, A. A. R., Pullen, A. M., Doughty, C. E., Metcalfe, D. B., Vasconcelos, S. S., Ferreira, L. V., Malhi, Y., Grace, J., Mencuccini, M., & Meir, P. (2015). Death from drought in tropical forests is triggered by hydraulics not carbon starvation. *Nature*, *528*, 119–122.

Rutuja, C.-T., Xu, C., Aguilar, S., Anderson-Teixeira, K. J., Chambers, J., Detto, M., Faybishenko, B., Fisher, R. A., Knox, R. G., Koven, C. D., Kueppers, L. M., Kunert, N., Kupers, S. J., McDowell, N. G., Newman, B. D., Paton, S. R., Pérez, R., Ruiz, L., Sack, L., … McMahon, S. M. (2021). Hydraulically-vulnerable trees survive on deep-water access during droughts in a tropical forest. *The New Phytologist*, *231*(5), 1798–1813.

Silveira, M., Daly, D. C., Salimon, C. I., Wadt, P., Amaral, E. F., Pereira, M. G., & Passos, V. (2008). Ambientes físicos e coberturas vegetais do Acre. *Primeiro Catálogo da flora do Acre, Brasil. Rio Branco, AC: EDUFAC*, 36–63.

Silvertown, J., Araya, Y., & Gowing, D. (2015). Hydrological niches in terrestrial plant communities: A review. *The Journal of Ecology*, *103*, 93–108.

Skelton, R. P., Dawson, T. E., Thompson, S. E., Shen, Y., Weitz, A. P., & Ackerly, D. (2018). Low vulnerability to xylem embolism in leaves and stems of north American oaks. *Plant Physiology*, *177*, 1066–1077.

Sorek, Y., Greenstein, S., Netzer, Y., Shtein, I., Jansen, S., & Hochberg, U. (2021). An increase in xylem embolism resistance of grapevine leaves during the growing season is coordinated with stomatal regulation, turgor loss point and intervessel pit membranes. *The New Phytologist*, *229*, 1955–1969.

Sousa, T. R., Schietti, J., Coelho de Souza, F., Esquivel-Muelbert, A., Ribeiro, I. O., Emílio, T., Pequeno, P. A. C. L., Phillips, O., & Costa, F. R. C. (2020). Palms and trees resist extreme drought in Amazon forests with shallow water tables. *The Journal of Ecology*, *108*, 2070–2082.

Sousa, T. R., Schietti, J., Ribeiro, I. O., Emílio, T., Fernández, R. H., ter Steege, H., Castilho, C. V., Esquivel-Muelbert, A., Baker, T., Pontes-Lopes, A., Silva, C. V. J., Silveira, J. M., Derroire, G., Castro, W., Mendoza, A. M., Ruschel, A., Prieto, A., Lima, A. J. N., Rudas, A., … Grytnes, J.-A. (2022). Water table depth modulates productivity and biomass across Amazonian forests. *Global Ecology and Biogeography: A Journal of Macroecology*, *31*, 1571–1588.

Sparks, J. P., & Black, R. A. (1999). Regulation of water loss in populations of *Populus trichocarpa*: The role of stomatal control in preventing xylem cavitation. *Tree Physiology*, *19*, 453–459.

Sperry, J. S. (2000). Hydraulic constraints on plant gas exchange. *Agricultural and Forest Meteorology*, *104*, 13–23.

Sperry, J. S., & Saliendra, N. Z. (1994). Intra-and inter-plant variation in xylem cavitation in *Betula occidentalis*. *Plant, Cell & Environment*, *17*, 1233–1241.

Tavares, J. V., Oliveira, R. S., Mencuccini, M., Signori-Müller, C., Pereira, L., Diniz, F. C., Gilpin, M., Marca Zevallos, M. J., Salas Yupayccana, C. A., Acosta, M., Pérez Mullisaca, F. M., Barros, F. D. V., Bittencourt, P., Jancoski, H., Scalon, M. C., Marimon, B. S., Oliveras Menor, I., Marimon, B. H., Jr., Fancourt, M., … Galbraith, D. R. (2023). Basin-wide variation in tree hydraulic safety margins predicts the carbon balance of Amazon forests. *Nature*, *617*, 111–117.

Trugman, A. T., Anderegg, L. D. L., Anderegg, W. R. L., Das, A. J., & Stephenson, N. L. (2021). Why is tree drought mortality so hard to predict? *Trends in Ecology & Evolution*, *36*, 520–532.

Urli, M., Porté, A. J., Cochard, H., Guengant, Y., Burlett, R., & Delzon, S. (2013). Xylem embolism threshold for catastrophic hydraulic failure in angiosperm trees. *Tree Physiology*, *33*, 672–683.

von Randow, C., Manzi, A. O., Kruijt, B., de Oliveira, P. J., Zanchi, F. B., Silva, R. L., Hodnett, M. G., Gash, J. H. C., Elbers, J. A., Waterloo, M. J., Cardoso, F. L., & Kabat, P. (2004). Comparative measurements and seasonal variations in energy and carbon exchange over forest and pasture in south West Amazonia. *Theoretical and Applied Climatology*, *78*, 5–26.

Wang, M., Ding, L., Gao, L., Li, Y., Shen, Q., & Guo, S. (2016). The interactions of aquaporins and mineral nutrients in higher plants. *International Journal of Molecular Sciences*, *17*, 1229.

Wright, I. J., Ackerly, D. D., Bongers, F., Harms, K. E., Ibarra-Manriquez, G., Martinez-Ramos, M., Mazer, S. J., Muller-Landau, H. C., Paz, H., Pitman, N. C. A., Poorter, L., Silman, M. R., Vriesendorp, C. F., Webb, C. O., Westoby, M., & Wright, S. J. (2007). Relationships among ecologically important dimensions of plant trait variation in seven neotropical forests. *Annals of Botany*, *99*, 1003–1015.

Zhang, Y., Lamarque, L. J., Torres-Ruiz, J. M., Schuldt, B., Karimi, Z., Li, S., Qin, D.-W., Bittencourt, P., Burlett, R., Cao, K.-F., Delzon, S., Oliveira, R., Pereira, L., & Jansen, S. (2018). Testing the plant pneumatic method to estimate xylem embolism resistance in stems of temperate trees. *Tree Physiology*, *38*, 1016–1025.

Zuquim, G., Stropp, J., Moulatlet, G. M., Van Doninck, J., Quesada, C. A., Figueiredo, F. O. G., Costa, F. R. C., Ruokolainen, K., & Tuomisto, H. (2019). Making the most of scarce data: Mapping soil gradients in data-poor areas using species occurrence records. *Methods in Ecology and Evolution/British Ecological Society*, *10*, 788–801.

Zwieniecki, M. A., & Secchi, F. (2015). Threats to xylem hydraulic function of trees under "new climate normal" conditions. *Plant, Cell & Environment*, *38*, 1713–1724.

SUPPORTING INFORMATION

Additional supporting information can be found online in the Supporting Information section at the end of this article.

How to cite this article: Garcia, M. N., Domingues, T. F., Oliveira, R. S., & Costa, F. R. C. (2023). The biogeography of embolism resistance across resource gradients in the Amazon. *Global Ecology and Biogeography*, *00*, 1–13. https://doi.org/10.1111/geb.13765